International Journal of Science and Research (IJSR)
ISSN: 2319-7064
SJIF (2022): 7.942

Green Synthesis of Iron Oxide Nanoparticles by Using *ALBIZIA AMARA* Leaf Extract and its Characterization and Antioxidant Studies

Sujatha Dadhala[1], Saraswathi Ramaiah Chinnasamy[2], Alvin Kalicharan Athiappan[3], Padma Muthu[4], Arivalagan Kuppusamy[5]

[1, 2, 5]Department of Chemistry, Government Arts College for Men (A), Chennai, Tamilnadu, India
Email: *arivualagan16[at]gmail.com*

[3]Department of chemistry, Panimalar Engineering College, Chennai, Tamilnadu, India
Email: *kalicharan19982[at]gmail.com*

[4]Department of Chemistry, Bharathi Womens College, Chennai, Tamilnadu, India
Email: *padmachembwc[at]gmail.com*

[5]Corresponding Author Email: *arivualagan16[at]gmail.com*

Abstract: ***Iron oxide nanoparticles, one of the metal oxide nanoparticles have different forms and properties. In recent years, iron oxide nanoparticles have been successfully synthesized from various plant species using green synthesis pathways and have been analysed for different biological properties. In this study, iron oxide nanoparticles were synthesized using an unconventional, eco - friendly and completely non - hazardous technique using Albiziaamara leaf extract as a reducer and stabilizing agent. The synthesized iron oxide nanoparticles were characterized using the Ultraviolet - visible spectrometer (UV - Vis), Fourier transform infrared spectroscopy (FT - IR), X - ray diffraction (XRD), Scanning electron microscopy (SEM), Energy dispersive X - ray (EDX), and Transmission electron microscopy (TEM). In addition, the antioxidant activity of the product was analysed and it was recorded that the nanoparticle has remarkable antioxidant activity.***

Keywords: green synthesis, iron oxide nanoparticles, *Albiziaamara* leaves extract, antioxidant activity

1. Introduction

In recent years have perceived a rising interest in the nano synthesis of environment friendly nanoparticles without involving the production of toxic by - products as part of the synthesis process [1 - 3]. Green chemistry synthesis methods for nanoparticles have optimistic aspects over conventional methods, for example being safe, eco - friendly, harmful compounds are not employed, mild reaction, easy operation and also cheap [4]. Green synthesis methods are as follows: Firstly, the dynamic biological component such as enzymes works as reducing and also as capping agents, and this is the reason why these small nanoparticles could be generated in the course of large - scale production [5], Secondly, the plant extracts also reduce the metal - ions in a short time, and it is broadly used because of the presence of reducing and stabilizing agents in their extracts [6] and Finally, an astonishingly wide range of natural resources such as germs (bacteria, thrush, fungi, algae and also viruses) and crops could be utilized intended for nanoparticle functionality [7].

The green synthesis methods mainly uses microorganisms, plants or plant parts extracts as a stabilizer and reducing agent respectively to synthesize nanoparticles. The feasibility of this path mainly lies in the amount of bioactive molecules such as proteins, amino acids or polysaccharides contained in microorganisms and active ingredients such as terpenoids, phenols, alkaloids, flavonoids, quinines or tannins contained in plant parts extract, which not only have antibacterial and antioxidant ability but also reduce metal salts and stabilize nanoparticles [8].

However the microbial - based synthesis, which has the drawbacks of time consumption on cultivation of bacteria or fungi, high cost and being prone to biosafety problems, is generally not applied [9]. In divergence, the plant - mediated synthesis method of nanoparticles featured with many advantages including being more rapid, cheap and simpler operation with more abundant resources [8] and has, therefore, received widespread attention from researchers around the world.

To make the plant extract, different parts of the plants are used as fresh or dry material such as fruit, leaf, peel, petal and shoot. The extraction procedure usually involves soaking the plant material in a green solvent with or without stirring followed by filtration and centrifugation. The filtered extract is rich in the reducing and capping agents required for the bio reduction of metallic ions. The advantages of using dried plant is that it has a long shelf life at room temperature, but it is important to store the fresh plant at 20^{o}C to avoid any deterioration. In addition, the use of dry plant material ensures the elimination of effects of seasonal variations leading to variations in plant constituents [10, 11].

One of the major applications of nanotechnology in chemistry is the synthesis of metal and metal oxide nanoparticles [12]. Metallic nanoparticles have attracted great attention in recent years and the best way for future generations because they possess exceptional characteristics such as optical properties, high surface area, surface plasmon resonance, mechanical strengths, low melting point,

magnetic properties and good antibacterial properties and hence have vast applications in different areas such as catalysis, photography, in medical field as antioxidant, anticancer and antimicrobial agents, biotechnology and agriculture [13, 14].

Out of these above mentioned metal oxides nanoparticles one of the preeminent biocompatible nanoparticles are iron oxides as they have magnificent minuscule physical characteristics like superpara magnetism (this is found only in iron nanoparticles), firmness in liquid solution, low susceptibility to oxidation, long blood half - lives, flexible surface chemistry with wide range of applications in environmental regulation like antibiotic degradation, adsorption of dyes, food related processes, biomedical, bioengineering, cosmetics and bio sensing along with antimicrobial activity against various pathogens like fungus and bacteria [15 - 18].

The present research was designed for the green synthesis of iron oxide nanoparticles from plant extract of *Albiziaamara* leaves and discussed.

2. Materials and methods

Malachite Green (MG), Alizarin Red (AR) and Safranin O (SO), $FeCl_3$, NaOH, H_2SO_4 and HCl were assimilated from Kevin Laboratories in Chennai. Mueller Hinton broth, Potato dextrose broth, Agar, Azithromycin, Clotrimazole, 2, 2 - diphenylpicrylhydrazyl (DPPH), methanol, hydrogen peroxide, sodium phosphate, ascorbic acid, sodium nitroprusside, Griess reagent, ammonium acetate, Nitro Blue Tetrazolium (NBT), Phenazine Methosulphate (PMS), 3 - (4, 5 - dimethylthiazol - 2 - yl) - 2, 5 - diphenyl tetrazolium bromide (MTT), Dulbecco's Modified Eagle Medium (DMEM), fetal bovine serum (FBS), dimethyl sulfoxide (DMSO), penicillin, streptomycin were purchased from Sigma - Aldrich. HeLa cervical cancer cells and HaCaT skin cells were acquired from the National Centre for Cell Science (NCCS), Pune, India. All the microorganisms were purchased from the Microbial Type Culture Collection and Gene Bank (MTCC), Chandigarh, India.

Preparation of Dye solution: Malachite Green (MG), Alizarin Red (AR) and Safranin O (SO) dyes were prepared in double distilled water to prepare stock solutions (1 gm of dye in 1000ml of double distilled water) of respective dyes. This stock solution was diluted, and new practicable solutions were created with the aid of 0.01N H_2SO_4 and 0.01N NaOH in order to alter the initial pH.

Preparation of *Albiziaamara*leaf extract: Fresh leaves of *Albiziaamara* were gathered from Kallakurichi, Tamilnadu, India and subjected to multiple washes using tap water and subsequently with distilled water to eliminate any dust particles. The washed leaves were cut into a small pieces then dried for a period of 5 to 10 days in a covered area at room temperature. Once completely dried, the leaves were pulverized in an electronic blender to obtain a fine powder, which was then stored in an air tight container at room temperature for future use.

For the extraction process, 10 grams of the obtained leaf powder was measured and placed in a 250 ml conical flask. To this 100 ml of double distilled water was added, and the mixture was heated at 80 to 90°C for 30 minutes. After the heating process, the solution was filtered through Whatman filter paper No.1 and allowed to cool at room temperature. The filtrate was centrifuged at 1200 rpm for 15 minutes, after which it was filtered, the pale brown solution was adjusted to a pH=11 by adding 0.1M of NaOH solution, and then set aside for further processing. .

Synthesis of Iron Oxide Nanoparticles: In a 250 ml conical flask, 50 ml of *Albiziaamara* leaves extract was taken and to this 100 ml of 0.1M $FeCl_3$ solution was gradually added at room temperature under static condition. The colour change was observed and the time taken for the reaction to occur was noted. As soon as iron oxide nanoparticles form, the colour of the solution changes from pale brownish to reddish brown. Further the solution was centrifuged and the obtained precipitate was dried in a hot air oven for 24 hours at 100ºC. The synthesized iron oxide nanoparticles kept in the muffle furnace at 350^{o}C for 4 hours.

3. Results and Discussion

Characterization of Green Synthesized Iron Oxide Nanoparticles

UV - Visible absorption studies

The formation of iron oxide nanoparticles was evidenced by the addition of aqueous ferric chloride solution to the leaf extract resulted in the appearance of an instantaneous dark black colour change from brown in the solution. This formation was due to a variety of plant biomolecules such as polyphenols, flavonoids, which played major role in the reduction of metal ions and sufficiently stabilized the iron oxide nanoparticles. The absorbance spectra of the solution were recorded at a 110 – 900 nm wavelength range. The formation of an SPR band was observed. Figure 1, shows the UV - Visible absorption spectra of the synthesized iron oxide nanoparticles and *Albiziaamara* leaf extract. The spectra demonstrated a characteristic peaks surface plasmon resonance band around 412 nm for iron oxide nanoparticles. The SPR arose from the collective oscillation of free electrons in the conduction band of iron oxide nanoparticles [19].

As can be seen from Figure 1a, the absorption peaks for *Albiziaamara* leaf extracts are around 370 to 390 nm, which corresponds to the existence of several natural compounds in the extracts [20]. These peaks are vanished after reacting with an iron salt, indicating that the extract compounds acted as reducing and capping agents to synthesize the iron oxide nanoparticles. Furthermore, and in accordance with the results of the present study, the surface plasmon band for iron oxide nanoparticles at wavelengths of 412 nm indicate the formation of iron oxide nanoparticles were reported by previous studies [21].

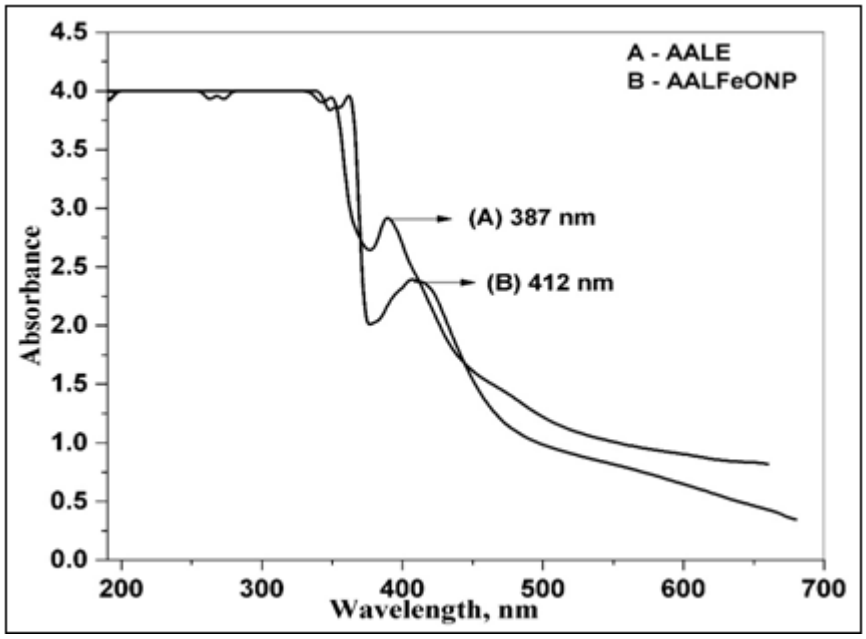

Figure 1: UV - Visible spectra of *Albiziaamara* leaf extract and iron oxide nanoparticles

By utilizing the Planck's equation, the band energy gap of iron oxide nanoparticles has been calculated from UV - Vis spectrum (Equation 1),

$$E_{bg} = 1240 / \lambda \text{ (eV)} \quad (1)$$

λ - absorption maximum wavelength (nm)

From the above formula the E_{bg} value of iron oxide nanoparticles was found to be 3.00 eV [22].

Structural analysis by FT - IR spectroscopy

FT - IR measurements were performed on the *Albiziaamara* leaf extract and the synthesized iron oxide nanoparticles to identify a possible change in functional group bonds during the reduction process and presented in Figure 2. The spectra revealed the presence of different functional groups in the biomolecules and their possible involvement in the synthesis and stabilization of the iron oxide nanoparticles.

Both spectra shows similar IR absorption bands confirming the presence of organic compounds from the *Albiziaamara* leaf extract at the surface of the iron oxide nanoparticles limiting their agglomeration. The bands were slightly shifted in the IR spectrum of iron oxide nanoparticles as compared to those that appeared in *Albiziaamara* leaf extract spectrum.

Figure 2a, shows the IR spectrum for *Albiziaamara* leaf extracts displayed prominent bands of absorbance at around 3391, 2069, 1639, 816 and 681 cm^{-1}. The same pattern was roughly observed for the synthesized iron oxide nanoparticles Figure 2b. The shifted absorption band observed at 561 cm^{-1}, for the *Albiziaamara* leaf extract band at 681 cm^{-1} corresponds to Fe - O stretches of iron oxide confirming the formation of nanoparticles. The observed bands were higher in intensity than the extract, confirming the reducing role of the extract in the formation of iron oxide nanoparticles. In Figure 2a, the peak near 1000 cm^{-1} corresponds to the stretching vibration of C - O - C, polyphenol compounds present in the plant extract. The absorption band at 1639 cm^{-1} related to the C=O bond stretching denotes polyphenol compounds and amino acids which stabilized and acted as a capping agent. Polyphenol compounds and phenyl groups play an essential role in reducing iron ions and then to iron oxide nanoparticles [23]. The band with higher intensity (Figure 2b) assigned to the - OH groups indicates water soluble polyphenol compounds that have capped the surface of the prepared iron oxide nanoparticles. The band at 2047 cm^{-1} may be due to C≡N stretching from unreacted impurities or due to CO_2 in the sample compartment. The band at 3393 cm^{-1} and 2800 cm^{-1} corresponds to the - OH bond stretching and denotes the aqueous phase, with an increase in the absorption band, indicating the ferrous sulphate reduction. The existing findings agreed well with the reported values [24].

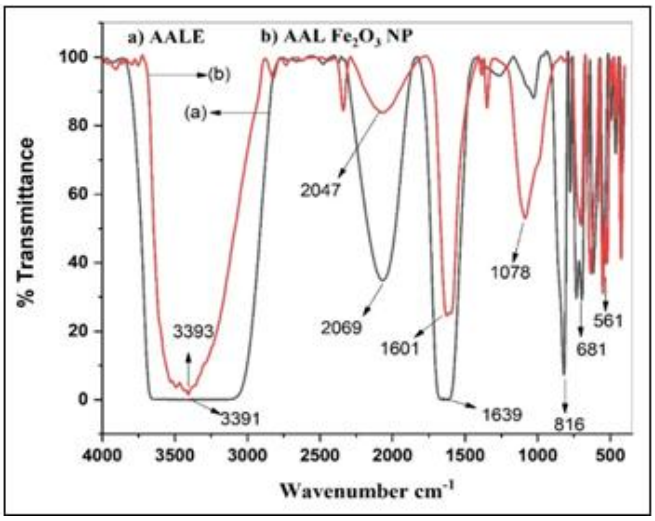

Figure 2: FT - IRspectra of a) *Albiziaamara* leaf extract and b) iron oxide nanoparticles

Crystallite calculation through X - ray diffraction (XRD) analysis

XRD is an exciting analysis commonly applied to determine the structural properties to ascertain the crystalline nature and phase identification of iron oxide nanoparticles. The XRD pattern of the *Albiziaamara* leaf extract stabilized iron oxide nanoparticles shown in Figure 3. The spectrum was recorded at a speed scan of 1 degree per minute in a 2 theta range of 20 – 80 degrees at an X - ray wavelength of 1.54

nm. The XRD data as shown in Figure 5.4 shows six distinct peaks at 2 θ values of 35.12°, 36.63°, 40.64°, 49.97°, 57.08° and 65.49° with corresponding lattice plane values at (104), (110), (113), (024), (116) and (300) respectively. The intense and sharp peaks undoubtedly revealed that iron oxide nanoparticles formed by the reduction method using *Albiziaamara* leaf extract were crystalline in nature. Furthermore, all these diffraction peaks are in good agreement with the database of standard ICPDS Card number 00 - 019 - 0629. The results are almost similar to the results obtained for iron oxide nanoparticles by other researchers [25 - 27].

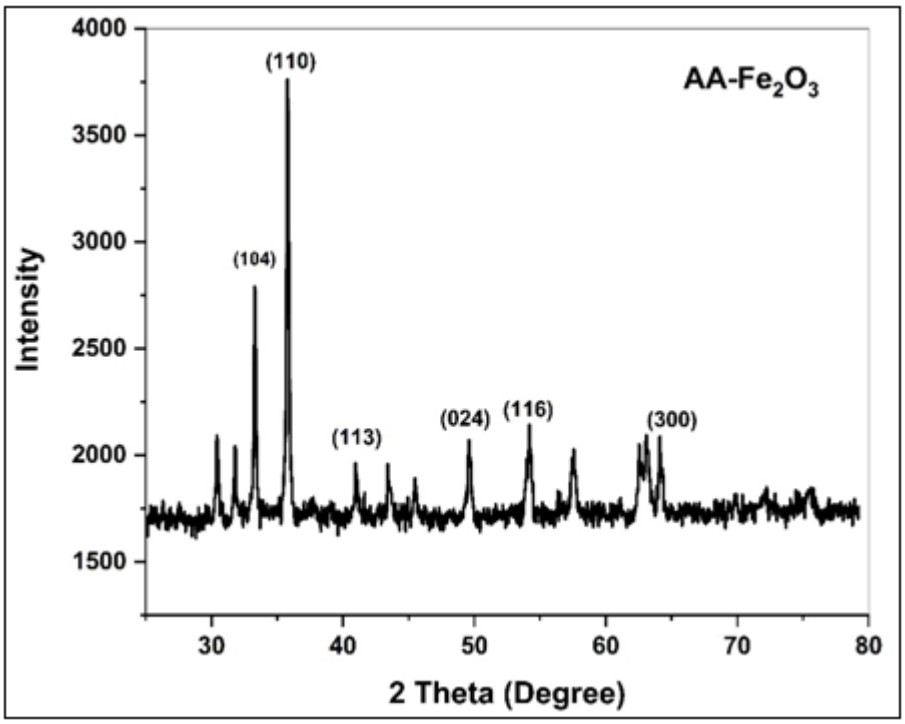

Figure 3: X - ray diffraction spectrum of iron oxide nanoparticles

Dynamic Light Scattering (DLS) studies

Photon correlation spectroscopy (PCS) or Quasi elastic light scattering (QELS), better termed as Dynamic light scattering was used to look into the size distribution aspects of the bioinspired iron oxide nanoparticles. Figure 4, shows the size of the colloidal iron oxide nanoparticles and their granulometric distribution has been recorded and expressed against the particle number and their intensity.

Biosynthesized iron oxide nanoparticles are dispersed in distilled water and sonicated for 30 minutes. Measurement condition is maintained with a refractive index of 1.3328 and viscosity of the dispersion is 0.899 (cP) at room temperature 25ºC. Narrow size distribution in the region of 180 – 280 nm shows the well size reduction by plant extract. More than 80% of the particles were of 200 nm [28].

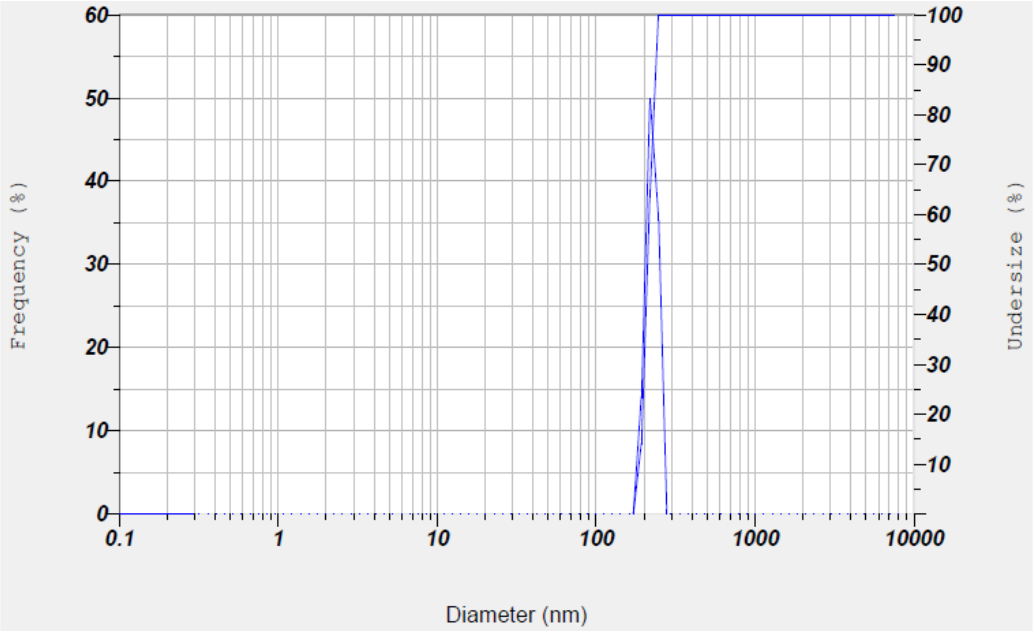

Figure 4: DLS plot for green synthesized iron oxide nanoparticles

SEM analysis and EDAX

SEM images provided further insight into the morphology and size details of the iron oxide nanoparticles. The morphology of the synthesized iron oxide nanoparticles is shown in Figure 5a - d. The images were recorded with magnification of 1 µm, 5 µm, 10 µm and 50 µm. The micrograph observations shows that the *Albiziaamara* leaf extract synthesized iron oxide nanoparticles are not uniform and, in some cases, agglomerated. The large agglomerated clusters were formed due to the accumulation of tiny building blocks of various bioactive reducing agents in plant extract or as a result of plant extracts lower capping ability and the agglomeration tendency of the iron - based nanoparticles due to magnetic interactions. The results are in agreement with the previous reports [29, 30].

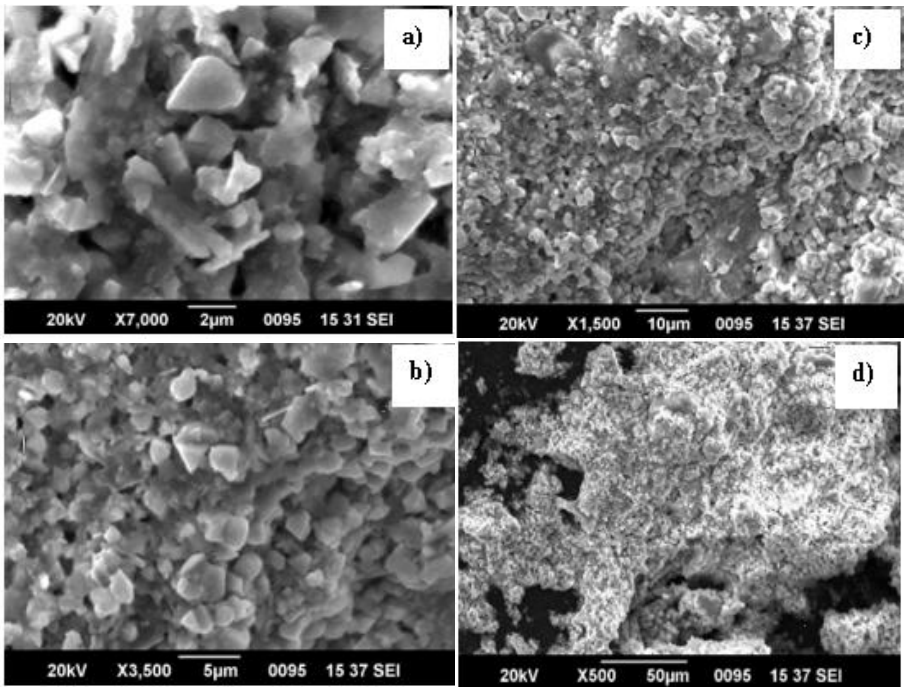

Figure 5: SEM images of green synthesized iron oxide nanoparticles (a – d)

The elemental composition of the green synthesized iron oxide nanoparticles was analysed by EDX analysis. The green synthesized iron oxide nanoparticles displayed structure absorbance in the range of 0.6 KeV to 6.4 KeV. The EDX analysis in Figure 6, clearly shows the presence of K - α lines at 6.4 KeV due to Fe atoms present in the nanoparticles and K - α lines at 0.6 KeV from O atoms and K - α lines at 2.7 from Cl peaks. Similar results were also obtained by previous studies [31]. Other tiny peaks, such as Keα lines at 0.24, 1.25 and 1.5 KeV are coming from Ca, Na and Al respectively. Presence of Cl as impurities is usually observed during iron oxide nanoparticles synthesized from ferric chloride as precursors. The analysis showed that the EDX spectrum containing intense peaks of O, Cl and Fe in addition to minor peaks Ca. Na and Al. The Fe and Cl peaks might have originated from the FeCl3 precursors used in the fabrication of these iron oxide nanoparticles. The Ca, Na and Al peaks could mainly have been due to the polyphenol groups or other sodium/aluminium containing molecules present in the *Albiziaamara* leaf extract. The higher percentage of chlorine indicated the plant biomolecules present in the metal ions reduction and stabilization of the green synthesized iron oxide nanoparticles [32]. The percent of weight and atomic weight percentage are listed in Table 1.

Table 1: Constituent elements and their percentage values

Element	Line type	Weight %	Atomic %
O	K series	23.05	46.61
Cl	K series	10.28	9.38
Ca	K series	7.40	5.98
Fe	K series	52.38	30.34

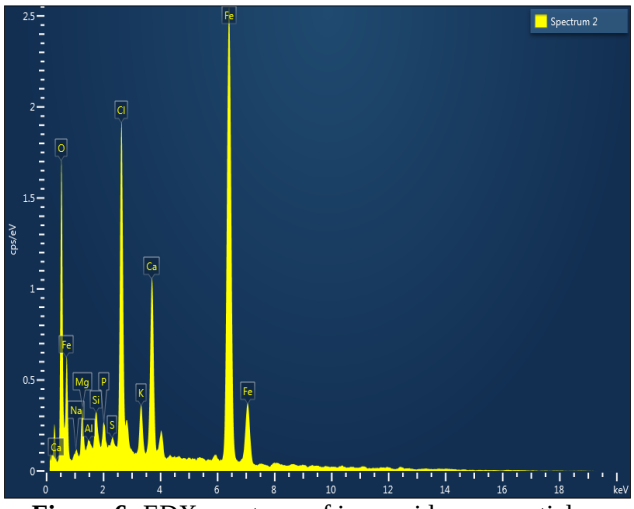

Figure 6: EDX spectrum of iron oxide nanoparticles

HR - TEM with SAED analysis

The application of TEM in nano sciences is significant to view the particles in nanoscale. TEM was performed to determine the shapes and sizes of iron oxide nanoparticles synthesized using *Albiziaamara* leaf extract. The sample was prepared for TEM imaging by disbanding drops of the iron oxide nanoparticle solution on a copper grid and left to dry at room temperature. The HR - TEM images of synthesized iron oxide nanoparticles and SAED pattern obtained from

HR - TEM studies are depicted in Figure 7a - d, which give clear indications regarding size, shape and size distribution of nanoparticles. Figure 7a, shows the TEM images of iron oxide nanoparticles which reveals a polydispersity in shapes and sizes, with most nanoparticles of nearly spherical in shape, which agrees with XRD analysis [29].

HR - TEM shows (Figure 7b) the crystalline structure of single biogenic nanoparticles, with visible lattice fringes with springe spacing of 0.20 nm was calculated, corresponding to the plane family (111) of FCC iron. The particle size distribution and average size distribution is calculated from the Gaussian fitting of size distribution histogram of as shown in Figure 7c. The particle size distribution of biogenic synthesized FeO NPs ranges from 100 to 200 nm, where the average particle size is found to be 160 nm.

Moreover, the selected area electron diffraction (SAED) pattern (Figure 7d), which indicates their cubic crystallinity nature and each of the diffraction rings has been indexed as (110), (113), (116) and (300). The SAED pattern of the single particle, the sharp diffraction spots (white dots in Figure 7d) clearly suggest the particle is of single crystal quality and the plane could be indexed to the FCC iron. The results are in agreement with XRD result as well.

From the Figure 7d, the crystalline nature of green synthesized iron oxide nanoparticles is confirmed by the presence of bright spots. The concentric bright rings encompassing of small spots (Figure 7d) proved that the green synthesized iron oxide nanoparticles were highly crystalline and those where of cubic crystalline. These characteristic concentric rings with tiny spots symbolised the presence of planes corresponding to iron oxide nanoparticles [33].

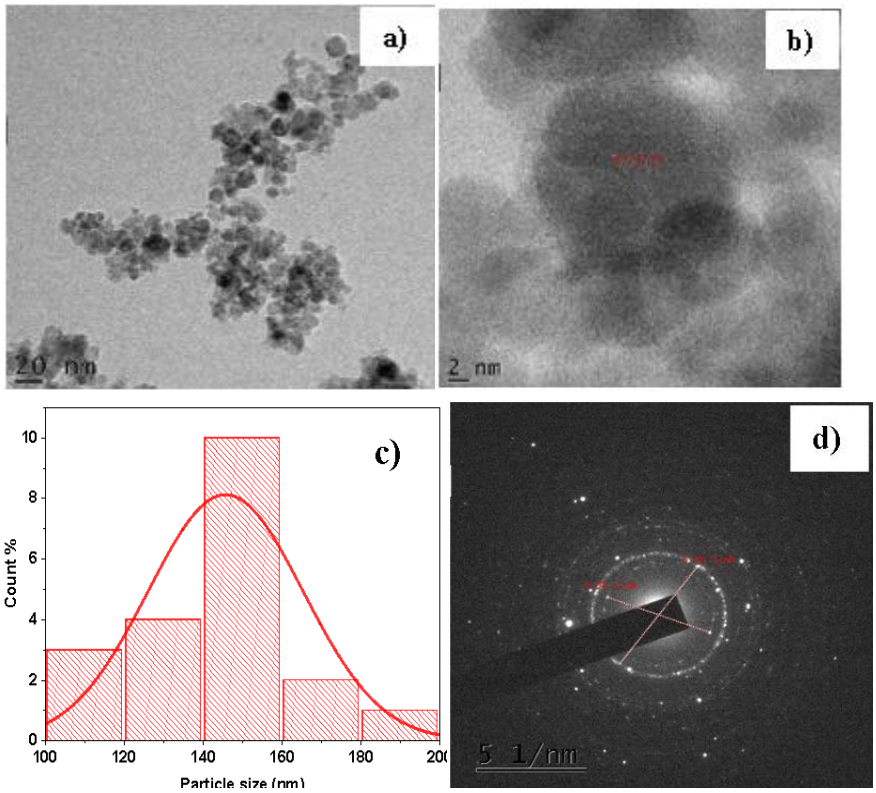

Figure 7: a) TEM image b) Particle size histogram c) HRTEM image and d) SAED pattern of green synthesized iron oxide nanoparticles

Antioxidant Potential of Green Synthesized Iron Nanoparticles

DPPH radical scavenging assay

Antioxidant potential of green synthesized iron oxide nanoparticles were normally inspected by 2, 2 - diphenyl - 1 - picrylhydrazyl (DPPH) method. Principle of this method is that DPPH reacts with proton donors like phenols and metal oxide nanoparticles. Here, the scavenging capability of antioxidant property owning bioactive compounds are evaluated. DPPH comprises of an odd electron of N atom that is abridged by receiving an H atom from antioxidants or metal oxide nanoparticles to particular hydrazine [34].

From the Figure 8, observed the upon treatment with iron oxide nanoparticles the purple colour of DPPH is changed to colourless. This proves the iron oxide nanoparticles with superior antioxidant property. Also, we envisaged that the intensity of colour is reduced more for higher dosage of iron oxide nanoparticles. This confirms the dose dependent antioxidant activity of iron oxide nanoparticles.

DPPH scavenging activity is calculated using Equation 2:

$$\% \text{ of DPPH scavenging} = \frac{\text{Control absorbance} - \text{Sample absorbance}}{\text{Control absorbance}} \text{ X } 100\ \% \quad (2)$$

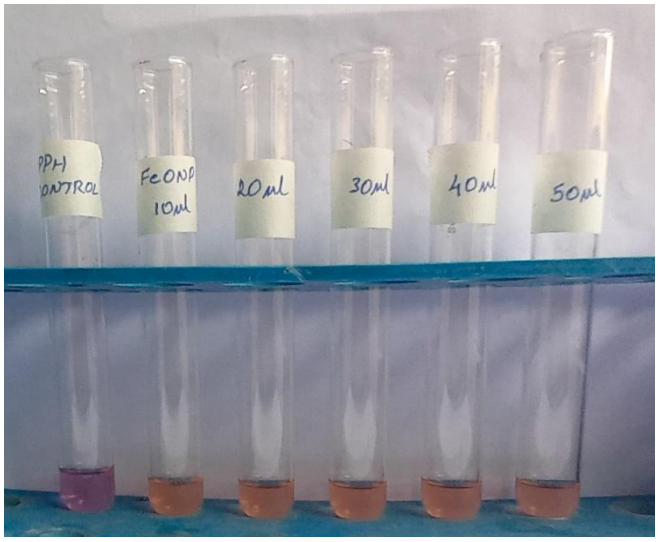

Figure 8: Decolourization of DPPH with the addition of green synthesized iron oxide nanoparticles

H_2O_2 radical scavenging assay

H_2O_2 is existing in atmosphere and in human body, flora and fauna at lower concentrations. It gets decayed to oxygen (O_2) and water (H_2O) and forms hydroxyl radicals (OH). This radical triggers DNA damage and cell death, hence it is important to inhibit the H_2O_2 with nanomaterials possessing antioxidant property. Presence of biomolecules in the iron oxide nanoparticles easily donates electrons to H_2O_2, thus neutralized into water. To screen the hydrogen peroxide inhibition using green synthesized iron oxide nanoparticles measurement of absorbance at 230 nm is carried out. The disappearance of H_2O_2 denotes the antioxidant property of iron oxide nanoparticles [34].

H_2O_2 scavenging action of iron oxide nanoparticles is shown in Figure9. It was found that the scavenging activity was dose dependent in nature.

H_2O_2 scavenging activity is calculated using Equation 3.

$$\% \text{ of } H_2O_2 \text{ scavenging} = \frac{\text{Control absorbance} - \text{Sample absorbance}}{\text{Control absorbance}} \text{ X } 100\ \% \quad (3)$$

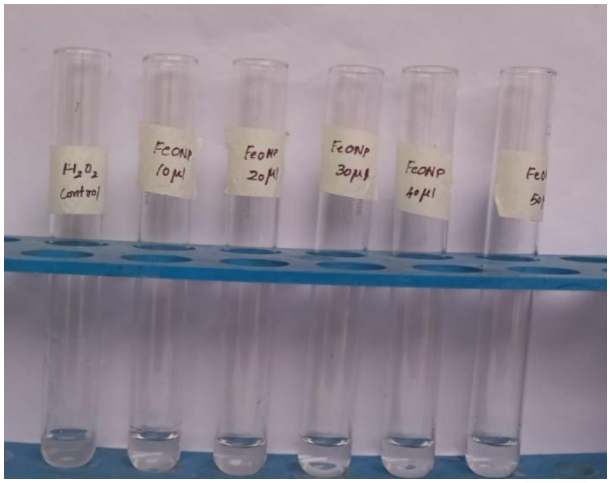

Figure 9: H_2O_2 radical scavenging assay using green synthesized iron oxide nanoparticles

Nitric oxide radical scavenging assay

Nitric oxide (NO) is an important molecule for signaling which has noteworthy role in the extent of swelling and immune based systems. When NO level is augmented it leads to swelling in the linkages, lungs and gut. Also numerous diseases are associated with enhanced NO production in body such as damage in vascular region. Generally, NO reacts with atmospheric oxygen to form a steady product such as nitrates and nitrite via intermediated like NO_2, N_2O_4 and N_3O_4. The toxic nature is further increased while it reacts with superoxide radical to produce next reactive component which is called as peroxynitrite anion ($ONOO^-$). [34]. NO scavenging assay is based on the reduction of absorbance at 550 nm which denotes the NO inhibition. From NO radical scavenging assay, we witnessed that the inhibition of NO as the concentration of iron oxide nanoparticles increased, thus denoting the dose - dependent antioxidant activity (Figure 10) [34].

NO scavenging activity is calculated using Equation 4:

$$\% \text{ of NO scavenging} = \frac{\text{Control absorbance} - \text{Sample absorbance}}{\text{Control absorbance}} \text{ X } 100\ \% \quad (4)$$

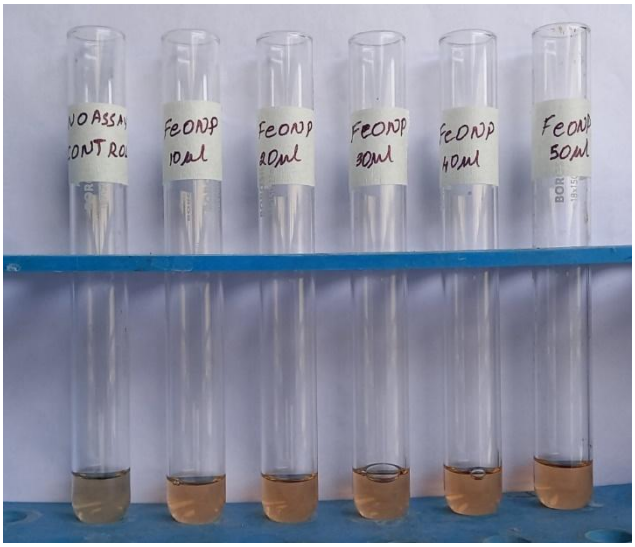

Figure 10: Nitric oxide radical scavenging assay using green synthesized iron oxide nanoparticles.

Superoxide Dismutase (SOD) radical scavenging assay

Superoxide dismutase (SOD) enzymes catalyzes the dismutation of SOD radical into hydrogen peroxide and molecular oxygen. Hence it is an important defense enzyme against superoxide radical toxicity. SOD enzyme is notable in fields such as cosmetology for anti - aging property by reducing the free radical damage to the body in order to protect from wrinkles and age spots. It aids protection in wound and scar treatment and also as UV filter. Figure 11, denotes the decolorization of SOD enzymes with the treatment of iron oxide nanoparticles in increased concentration denoting the dose - dependent antioxidant activity. The absorbance value has decreased with increase in concentration of iron oxide nanoparticles resulting in better SOD inhibition rate [34].

SOD scavenging activity is calculated using Equation 5:

$$\% \text{ of SOD scavenging} = \frac{\text{Control absorbance} - \text{Sample absorbance}}{\text{Control absorbance}} \text{ X } 100\ \% \quad (5)$$

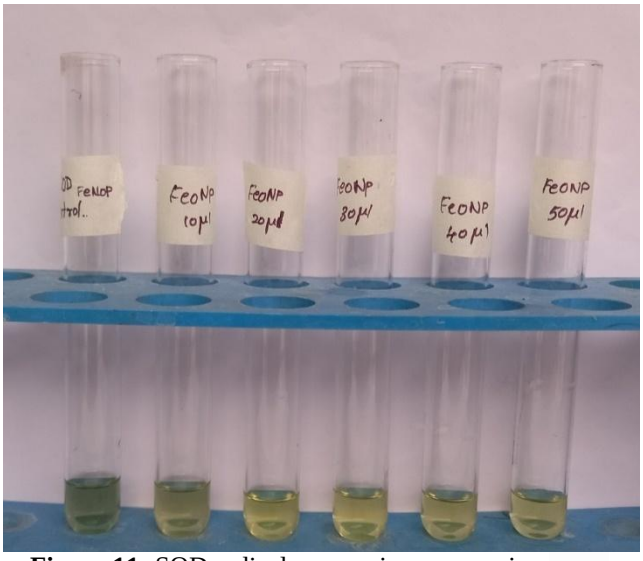

Figure 11: SOD radical scavenging assay using green synthesized iron oxide nanoparticles.

At higher concentration of iron oxide nanoparticles, the scavenging activity was higher for SOD assay followed by DPPH, NO and H_2O_2 assays with percentage of inhibition, 66.02 %, 62.13 %, 28.23 % and 22.77 %, respectively.

References

[1] Saratale R. G, Saratale G. D, Shin H. S, Jacob J. M, Pugazhendhi A, Bhaisare M and G. Kumar, "New insights on the green synthesis of metallic nanoparticles using plant and waste biomaterials: current knowledge, their agricultural and environmental applications, " Environ. Sci. Pollut. Res. Int.2018; 25: 10164 - 10183.

[2] Patra J. K and Baek K. H, "Green Nanobiotechnology: Factors Affecting Synthesis and Characterization Techniques, "J. of Nanomat.2014; 1 - 12.

[3] Shah M, Faweett D, Sharma S, Tripathy S. K and Poinern G. E, "Green Synthesis of Metallic Nanoparticles via Biological Entities, "Materials (Basel), 2015; 8: 7278 - 7308.

[4] Senapati S, Ahmad A, Khan M. L, Sastry M and Kumar R, "Extracellular Biosynthesis of Bimetallic Au - Ag Alloy Nanoparticles, "Small, 2005; 1: 517 - 520.

[5] Santhoshkumar J, Rajeshkumar S and Kumar S. V, "Phyto - assisted synthesis, characterization and applications of gold nanoparticles – A review, "Biochem. Biophys. Rep.2017; 11: 46 - 57.

[6] Rai M, Yadav A and Gade A, "CRC 675—Current Trends in Phytosynthesis of Metal Nanoparticles, " Critical Rev. in Biotech.2008; 28: 277 - 284.

[7] Mohanpuria P, Rana N. K and Yadav S. K, "Biosynthesis of nanoparticles: technological concepts and future applications, " J. of Nanopart. Res.2008; 10: 507 - 517.

[8] Narayanan K. B and Sakthivel N, "Green synthesis of biogenic metal nanoparticles by terrestrial and aquatic phototrophic and heterotrophic eukaryotes and biocompatible agents, " Adv. In Colloi. and Interf. Sci. 2011; 169: 59 - 79.

[9] Kumar V and Yadav S. K, "Plant - mediated synthesis of silver and gold nanoparticles and their applications, " J. of Chem. Tech. and Biotech.2009; 84: 151 - 157.

[10] Ingle K. P, Deshmukh A. G, Padole D. A, Dudhare M. S, Moharil M. P and Vaibhav K. C, "Phytochemicals: Extraction methods, identification and detection of bioactive compounds from plant extracts, " J. of Pharmacogn. Phytochem.2017; 6: 32 - 36.

[11] Altemimi A, Lakhssassi N, Baharlouei A, Watson D. G and Lightfoot D. A, "Phytochemicals: Extraction, Isolation, and Identification of Bioactive Compounds from Plant Extracts, " Plants (Basel), 2017; 6: 42.

[12] Rotello V. M, Springer Science & Business Media: New York, USA, 2004.

[13] Sulaiman G. M, Ali E. H, Jabbar I. I and Saleem A. H, "Synthesis, characterization, antibacterial and cytotoxic effects of silver nanoparticles, " Dig. J. of Nanomater. Biostruct.2014; 9: 787 - 796.

[14] He X and Hwang H. M, "Nanotechnology in food science: functionality, applicability, and safety assessment, " J. of Food Drug Anal.2016; 24: 671 - 681.

[15] Khalil A. T, Ovais M, Ullah I, Ali M, Shinwari Z. K and Maaza M, "Biosynthesis of iron oxide (Fe2O3) nanoparticles via aqueous extracts of Sageretiathea (Osbeck.) and their pharmacognostic properties, " Green. Chem. Lett. Rev.2017; 10: 186 - 201.

[16] Sruthi P. D, Sahithya C. S, Justin C, SaiPriya C, Bhavya K. S and Senthilkumar P, "Utilization of chemically synthesized super paramagnetic iron oxide nanoparticles in drug delivery, imaging and heavy metal removal, " J. of Cluster Sci.2019; 30: 11 - 24.

[17] Gao L, Fan K and Yan X, "Iron oxide Nanozyme: A multifunctional enzyme mimetics for biomedical application, " Nanozymology.2020; 105 - 140.

[18] Sharma P, Kumari S, Ghosh D, Yadav V, Vij A and Rawat P, "Capping agent - induced variation of physiochemical and biological properties of α - Fe_2O_3 nanoparticles, " Mater. Chem. Phys.2021; 258: 123899.

[19] Haiss W, Nguyen T. K, Aveyard T. J and Fernig D. G, "Determination of size and concentration of gold nanoparticles from UV - Vis spectra, " Analt. Chem.2007; 79: 4215 - 4221.

[20] Buarki F, AbuHassan H, Al Hannan F and Henari F. Z, "Green synthesis of iron oxide nanoparticles using hibiscus rosasinensis flowers and their antibacterial activity, " J. of Nanotechnol., 20222022; 2022: 1 - 6.

[21] Mahdavi M, Namvar F, Ahmad M. B and Mohmad R, "Green Biosynthesis and Characterization of Magnetic Iron Oxide (Fe3O4) Nanoparticles Using Seaweed (Sargassum muticum) Aqueous Extract, " Molecul. (2013; 18: 5954 - 5964.

[22] Das D, Nath B. C, Phukon P, Kalits A and Douli S. K, "Synthesis of ZnO Nanoparticles and Evaluation of Antioxidant and Cytotoxic Activity, " Colloids Surf. BBiointer.2013; 111: 556 - 560.

[23] Yardily A and Sunitha N, "Green synthesis of iron nanoparticles using hibiscus leaf extract, characterization, antimicrobial activity, " Inter. J. of Sci. Res. and Revie.2019; 8: 32 - 46.

[24] Demirezen D. A, Yilmaz S and Yilmaz D. D, "Green synthesis and characterization of iron nanoparticles using Aesculus hippocastanum seed extract, " Inter. J. of Adv. in Sci. Engg. and Tech.2018; 62: 24 - 29.
[25] Ahmmad B, Leonard K, Islam S, Kurawaki J, Muruganandham M, Ohkubo T and Kuroda Y, "Green synthesis of mesoporous hematite (α - Fe_2O_3) nanoparticles and their photocatalytic activity, " Adv. Power Technol.2013; 24: 160 - 167.
[26] Lassoued A, Lassoued M. S, Dkhil B, Ammar S and Gadri A, "Photocatalytic degradation of methylene blue dye by iron oxide (α - Fe_2O_3) nanoparticles under visible irradiation, Journal of material science, materials in electronics, " 2018: 29: 8142 - 8152.
[27] Suresh S, Karthikeyan S and Jayamoorthy K, "Effect of bulk and nano - Fe_2O_3 particles on peanut plant leaves studied by Fourier transform infrared spectral studies, " J. Adv. Res.2016; 7: 739 - 747.
[28] Stetefeld J, McKenna S. A and Patel T. R, "Dynamic light scattering: a practical guide and applications in biomedical sciences, " Biophysical Rev.2016; 8: 409 - 427.
[29] Newbury D. E, "Mistakes Encountered during Automatic Peak Identification in Low Beam Energy X - ray Microanalysis, " Scanning.2007; 29: 137 - 151.
[30] Md. Bhuiyan S. H, Miah M. Y, Paul S. C, Aka T. D, Saha O, Md. Rahaman M, Md. Sharif J. I, Habiba O and Md. Ashaduzzaman, "Green synthesis of iron oxide nanoparticle using *Carica papaya* leaf extract: application for photocatalytic degradation of remazol yellow RR dye and antibacterial activity, "Heliyon. 2020; 6: 1 - 13.
[31] Kiwumulo H. F, Muwonge H, Ibingira C, Lubwama M, Kirabira J. B and Ssekitoleko R. T, "Green synthesis and characterization of iron - oxide nanoparticles using Moringa oleifera: a potential protocol for use in low and middle income countries, "BMC Res. Notes.2022; 15: 149 - 157.
[32] Qasim, S, Zafar A, Saif, M. S, Ali Z, Nazar M, Waqas M, Haq A. U, Tariq T, Hassan S. G, Iqbal F, Shu X. G and Hasan M, "Green synthesis of iron oxide nanorods using Withaniacoagulans extract improved photocatalytic degradation and antimicrobial activity, " J. Photochem. Photobiol. B: Biology.2020; 204: 111784.
[33] Swathi Pon S. S and George M, "In vitro anticancer and antitubercular activities of cellulose - magnetite nanocomposite synthesized using deep eutectic solvent as a dispersant, " J. Mater. Nano Sci.2021; 8: 1 - 10.
[34] Tabassum N, Singh V, Chaturvedi, V. K, Vamanu E, Singh V, Singh M. P, "A Facile Synthesis of Flower - like Iron Oxide Nanoparticles and Its Efficacy Measurements for Antibacterial, Cytotoxicity and Antioxidant Activity, " Pharmaceutics, 2023; 15: 1726.